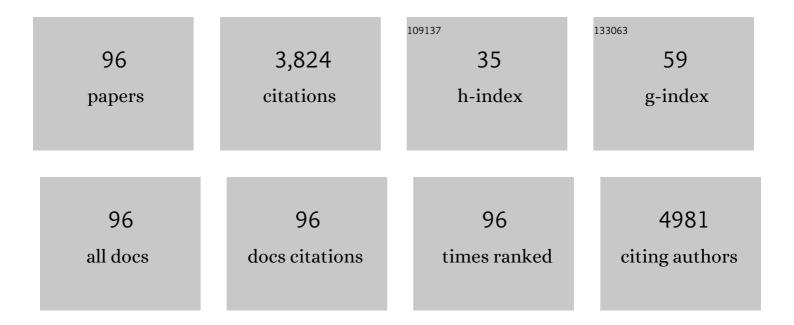
## List of Publications by Year in descending order

Source: https://exaly.com/author-pdf/4484041/publications.pdf

Version: 2024-02-01



Lii Li

#	Article	IF	CITATIONS
1	A Rapid Microwaveâ€Assisted Thermolysis Route to Highly Crystalline Carbon Nitrides for Efficient Hydrogen Generation. Angewandte Chemie - International Edition, 2016, 55, 14693-14697.	7.2	335
2	A Rapid Microwaveâ€Assisted Thermolysis Route to Highly Crystalline Carbon Nitrides for Efficient Hydrogen Generation. Angewandte Chemie, 2016, 128, 14913-14917.	1.6	234
3	New Ti 3 C 2 aerogel as promising negative electrode materials for asymmetric supercapacitors. Journal of Power Sources, 2017, 364, 234-241.	4.0	205
4	Two-color imaging of microRNA with enzyme-free signal amplification via hybridization chain reactions in living cells. Chemical Science, 2016, 7, 1940-1945.	3.7	202
5	Simultaneous Imaging of Zn <sup>2+</sup> and Cu <sup>2+</sup> in Living Cells Based on DNAzyme Modified Gold Nanoparticle. Analytical Chemistry, 2015, 87, 4829-4835.	3.2	138
6	A bismuth oxide nanosheet-coated electrospun carbon nanofiber film: a free-standing negative electrode for flexible asymmetric supercapacitors. Journal of Materials Chemistry A, 2016, 4, 16635-16644.	5.2	124
7	Ag-Nanoparticle-Decorated 2D Titanium Carbide (MXene) with Superior Electrochemical Performance for Supercapacitors. ACS Sustainable Chemistry and Engineering, 2018, 6, 7442-7450.	3.2	120
8	Flexible Ti <sub>3</sub> C <sub>2</sub> T <sub>x</sub> /PEDOT:PSS films with outstanding volumetric capacitance for asymmetric supercapacitors. Dalton Transactions, 2019, 48, 1747-1756.	1.6	119
9	In suit constructing 2D/1D MgIn2S4/CdS heterojunction system with enhanced photocatalytic activity towards treatment of wastewater and H2 production. Journal of Colloid and Interface Science, 2020, 576, 264-279.	5.0	109
10	Self-assembled Ti3C2Tx/SCNT composite electrode with improved electrochemical performance for supercapacitor. Journal of Colloid and Interface Science, 2018, 511, 128-134.	5.0	107
11	Highly Sensitive and Homogeneous Detection of Membrane Protein on a Single Living Cell by Aptamer and Nicking Enzyme Assisted Signal Amplification Based on Microfluidic Droplets. Analytical Chemistry, 2014, 86, 5101-5107.	3.2	92
12	Fluorescence Imaging of Intracellular Telomerase Activity Using Enzyme-Free Signal Amplification. Analytical Chemistry, 2016, 88, 12177-12182.	3.2	92
13	Molybdenum-doped CuO nanosheets on Ni foams with extraordinary specific capacitance for advanced hybrid supercapacitors. Journal of Materials Science, 2020, 55, 2492-2502.	1.7	74
14	Hemimicelle capped functionalized carbon nanotubes-based nanosized solid-phase extraction of arsenic from environmental water samples. Analytica Chimica Acta, 2009, 631, 182-188.	2.6	72
15	Novel Li <sub>x</sub> SiS <sub>y</sub> /Nafion as an artificial SEI film to enable dendrite-free Li metal anodes and high stability Li–S batteries. Journal of Materials Chemistry A, 2020, 8, 8979-8988.	5.2	72
16	In situ polymerized Ti3C2Tx/PDA electrode with superior areal capacitance for supercapacitors. Journal of Alloys and Compounds, 2019, 778, 858-865.	2.8	63
17	Multicolor Fluorescence Detection-Based Microfluidic Device for Single-Cell Metabolomics: Simultaneous Quantitation of Multiple Small Molecules in Primary Liver Cells. Analytical Chemistry, 2016, 88, 8610-8616.	3.2	62
18	FRET-Based Biofriendly Apo-GO <i><sub>x</sub></i> -Modified Gold Nanoprobe for Specific and Sensitive Glucose Sensing and Cellular Imaging. Analytical Chemistry, 2013, 85, 9721-9727.	3.2	58

#	Article	IF	CITATIONS
19	microRNA-199a-3p, DNMT3A, and aberrant DNA methylation in testicular cancer. Epigenetics, 2014, 9, 119-128.	1.3	57
20	Highly Sensitive Fluorescence Imaging of Zn <sup>2+</sup> and Cu <sup>2+</sup> in Living Cells with Signal Amplification Based on Functional DNA Self-Assembly. Analytical Chemistry, 2018, 90, 8785-8792.	3.2	56
21	Three-dimensional porous ZnCo2O4 sheet array coated with Ni(OH)2 for high-performance asymmetric supercapacitor. Journal of Colloid and Interface Science, 2017, 497, 50-56.	5.0	55
22	Simultaneous Quantitation of Na <sup>+</sup> and K <sup>+</sup> in Single Normal and Cancer Cells Using a New Near-Infrared Fluorescent Probe. Analytical Chemistry, 2015, 87, 6057-6063.	3.2	54
23	Visible/near-IR-light-driven TNFePc/BiOCl organic–inorganic heterostructures with enhanced photocatalytic activity. Dalton Transactions, 2016, 45, 9497-9505.	1.6	47
24	Consecutive Gated Injection-Based Microchip Electrophoresis for Simultaneous Quantitation of Superoxide Anion and Nitric Oxide in Single PC-12 Cells. Analytical Chemistry, 2016, 88, 930-936.	3.2	46
25	One-step synthesis of few-layer niobium carbide MXene as a promising anode material for high-rate lithium ion batteries. Dalton Transactions, 2019, 48, 14433-14439.	1.6	45
26	Progress of Twoâ€Dimensional Ti <sub>3</sub> C <sub>2</sub> T <sub><i>x</i></sub> in Supercapacitors. ChemSusChem, 2020, 13, 1296-1329.	3.6	45
27	The influence of the antiferromagnetic boundary on the magnetic property of La2NiMnO6. Applied Physics Letters, 2009, 95, .	1.5	42
28	Single-Cell Phenotypic Profiling of CTCs in Whole Blood Using an Integrated Microfluidic Device. Analytical Chemistry, 2019, 91, 11078-11084.	3.2	41
29	Hierarchical assembly of BiOCl nanosheets onto bicrystalline TiO2 nanofiber: Enhanced photocatalytic activity based on photoinduced interfacial charge transfer. Journal of Colloid and Interface Science, 2014, 435, 26-33.	5.0	40
30	Efficient extraction and preparative separation of four main isoflavonoids from Dalbergia odorifera T. Chen leaves by deep eutectic solvents-based negative pressure cavitation extraction followed by macroporous resin column chromatography. Journal of Chromatography B: Analytical Technologies in the Biomedical and Life Sciences, 2016, 1033-1034, 40-48.	1.2	40
31	A Near-Infrared Probe for Specific Imaging of Lipid Droplets in Living Cells. Analytical Chemistry, 2022, 94, 4881-4888.	3.2	40
32	A Rapid and Ultrasensitive Tetraphenylethylene-Based Probe with Aggregation-Induced Emission for Direct Detection of α-Amylase in Human Body Fluids. Analytical Chemistry, 2018, 90, 13775-13782.	3.2	39
33	Accurate <i>In Situ</i> Monitoring of Mitochondrial H <sub>2</sub> O <sub>2</sub> by Robust SERS Nanoprobes with a Au–Se Interface. Analytical Chemistry, 2021, 93, 4059-4065.	3.2	39
34	Quantitative Counting of Single Fluorescent Molecules by Combined Electrochemical Adsorption Accumulation and Total Internal Reflection Fluorescence Microscopy. Analytical Chemistry, 2008, 80, 3999-4006.	3.2	37
35	Simultaneous Single-Cell Analysis of Na <sup>+</sup> , K <sup>+</sup> , Ca <sup>2+</sup> , and Mg <sup>2+</sup> in Neuron-Like PC-12 Cells in a Microfluidic System. Analytical Chemistry, 2017, 89, 4559-4565.	3.2	36
36	Single-cell analyses highlight the proinflammatory contribution of C1q-high monocytes to Behçet's disease. Proceedings of the National Academy of Sciences of the United States of America, 2022, 119, .	3.3	35

#	Article	IF	CITATIONS
37	One-dimensional Ag <sub>3</sub> PO <sub>4</sub> /TiO <sub>2</sub> heterostructure with enhanced photocatalytic activity for the degradation of 4-nitrophenol. RSC Advances, 2015, 5, 29693-29697.	1.7	31
38	Ti3C2Tx-foam as free-standing electrode for supercapacitor with improved electrochemical performance. Ceramics International, 2018, 44, 13901-13907.	2.3	31
39	Imprinted propyl gallate electrochemical sensor based on graphene/single walled carbon nanotubes/sol–gel film. Food Chemistry, 2015, 177, 37-42.	4.2	29
40	An accurate mass spectrometric approach for the simultaneous comparison of GSH, Cys, and Hcy in LO2 cells and HepG2 cells using new NPSP isotope probes. Chemical Communications, 2015, 51, 11317-11320.	2.2	28
41	Performance evaluation of asymmetric supercapacitor based on Ti3C2Tx-paper. Journal of Alloys and Compounds, 2017, 729, 1165-1171.	2.8	26
42	Tailoring the Spatial Distribution and Content of Inorganic Nitrides in Solid–Electrolyte Interphases for the Stable Li Anode in Li–S Batteries. Energy and Environmental Materials, 2022, 5, 1180-1188.	7.3	26
43	Fluorescent sensing of pyrophosphate anion in synovial fluid based on DNA-attached magnetic nanoparticles. Biosensors and Bioelectronics, 2015, 72, 51-55.	5.3	25
44	Short-term effects of fine particulate matter on non-accidental and circulatory diseases mortality: A time series study among the elder in Changchun. PLoS ONE, 2018, 13, e0209793.	1.1	25
45	A high-performance supercapacitor electrode based on freestanding N-doped Ti3C2Tx film. Ceramics International, 2020, 46, 21482-21488.	2.3	25
46	Anaerobic caproate production on carbon chain elongation: Effect of lactate/butyrate ratio, concentration and operation mode. Bioresource Technology, 2021, 329, 124893.	4.8	25
47	Visible Light-Driven Self-Powered Device Based on a Straddling Nano-Heterojunction and Bio-Application for the Quantitation of Exosomal RNA. ACS Nano, 2019, 13, 1817-1827.	7.3	24
48	An Aggregationâ€induced Emission Probe Based on Host–Guest Inclusion Composed of the Tetraphenylethylene Motif and γâ€Cyclodextrin for the Detection of αâ€Amylase. Chemistry - an Asian Journal, 2019, 14, 847-852.	1.7	21
49	A High-Fidelity Electrochemical Platform Based on Au–Se Interface for Biological Detection. Analytical Chemistry, 2020, 92, 5855-5861.	3.2	20
50	A dual-responsive probe for the simultaneous monitoring of viscosity and peroxynitrite with different fluorescence signals in living cells. Chemical Communications, 2022, 58, 5976-5979.	2.2	20
51	New Strategy for Circumventing the Limitation of Thermally Linked States and Boosting the Relative Thermal Sensitivity of Luminescence Ratiometric Thermometry. Journal of Physical Chemistry C, 2019, 123, 6176-6181.	1.5	19
52	Multiple-mRNA-controlled and heat-driven drug release from gold nanocages in targeted chemo-photothermal therapy for tumors. Chemical Science, 2021, 12, 12429-12436.	3.7	18
53	Sputum-Based Tumor Fluid Biopsy: Isolation and High-Throughput Single-Cell Analysis of Exfoliated Tumor Cells for Lung Cancer Diagnosis. Analytical Chemistry, 2021, 93, 10477-10486.	3.2	18
54	Porous Co3O4 nanosheets as a high-performance non-enzymatic sensor for glucose detection. Analytical and Bioanalytical Chemistry, 2018, 410, 7663-7670.	1.9	17

#	Article	IF	CITATIONS
55	Responsive Dual-Targeting Exosome as a Drug Carrier for Combination Cancer Immunotherapy. Research, 2021, 2021, 9862876.	2.8	17
56	Multi-Functional Radar Waveform Generation Based on Optical Frequency-Time Stitching Method. Journal of Lightwave Technology, 2021, 39, 458-464.	2.7	16
57	Consecutive Sorting and Phenotypic Counting of CTCs by an Optofluidic Flow Cytometer. Analytical Chemistry, 2019, 91, 14133-14140.	3.2	15
58	ROS-mediated NLRP3 inflammasome activation participates in the response against Neospora caninum infection. Parasites and Vectors, 2020, 13, 449.	1.0	15
59	Effects of annealing time on structure and properties of sweet potato starch. Cereal Chemistry, 2020, 97, 573-580.	1.1	15
60	AtWAKL10, a Cell Wall Associated Receptor-Like Kinase, Negatively Regulates Leaf Senescence in Arabidopsis thaliana. International Journal of Molecular Sciences, 2021, 22, 4885.	1.8	14
61	Asymmetric supercapacitors with excellent rate performance by integrating Co(OH)F nanorods and layered Ti <sub>3</sub> C <sub>2</sub> T <sub>x</sub> paper. RSC Advances, 2019, 9, 30957-30963.	1.7	13
62	Bimetal Networked Nanosheets Co x Ni 3â^'x S 2 as An Efficient Electrocatalyst for Hydrogen Evolution. ChemCatChem, 2020, 12, 609-614.	1.8	13
63	CoS nanowires grown on Ti3C2Tx are promising electrodes for supercapacitors: High capacitance and remarkable cycle capability. Journal of Colloid and Interface Science, 2021, 602, 123-130.	5.0	13
64	Promoting effect of MXenes on 1T/2H–MoSe <sub>2</sub> for hydrogen evolution. CrystEngComm, 2021, 23, 4752-4759.	1.3	13
65	POMCPs with Novel Two Waterâ€Assisted Proton Channels Accommodated by MXenes for Asymmetric Supercapacitors. Small, 2022, 18, .	5.2	13
66	Phenotype-related drug sensitivity analysis of single CTCs for medicine evaluation. Chemical Science, 2020, 11, 8895-8900.	3.7	12
67	Dynamic fluorescent imaging analysis of mitochondrial redox in single cells with a microfluidic device. Biosensors and Bioelectronics, 2019, 129, 132-138.	5.3	11
68	One-pot synthesis of aminated cellulose nanofibers by "biological grinding―for enhanced thermal conductivity nanocomposites. Carbohydrate Polymers, 2021, 254, 117310.	5.1	11
69	The role of StAR2 gene in testicular differentiation and spermatogenesis in Nile tilapia (Oreochromis) Tj ETQq1	1 0.784314 1.2	4 rgBT /Overlo
70	Association between congenital heart defects and maternal manganese and iron concentrations: a case–control study in China. Environmental Science and Pollution Research, 2022, 29, 26950-26959.	2.7	11
71	Selective and Colorimetric Detection of p-Nitrophenol Based on Inverse Opal Polymeric Photonic Crystals. Polymers, 2020, 12, 83.	2.0	10
72	Diethylamine fluorescence sensor based on silica hollow sphere photonic crystals. Analytical Methods, 2021, 13, 2189-2195.	1.3	10

#	Article	lF	CITATIONS
73	Physicochemical Properties and Structure of Annealed Sweet Potato Starch: Effects of Enzyme and Ultrasound. Starch/Staerke, 2020, 72, 1900247.	1.1	8
74	Endochondral ossification pathway genes and postmenopausal osteoporosis: Association and specific allele related serum bone sialoprotein levels in Han Chinese. Scientific Reports, 2015, 5, 16783.	1.6	7
75	Synergistic effect of cocatalytic NiSe <sub>2</sub> on stable 1T-MoS <sub>2</sub> for hydrogen evolution. RSC Advances, 2021, 11, 6842-6849.	1.7	7
76	Heterogeneous Ru/TiO <sub>2</sub> for hydroaminomethylation of olefins: multicomponent synthesis of amines. Green Chemistry, 2021, 23, 2722-2728.	4.6	6
77	Kinetics of the Photoelectron-Transfer Process Characterized by Real-Time Single-Molecule Fluorescence Imaging on Individual Photocatalyst Particles. ACS Catalysis, 2021, 11, 6872-6882.	5.5	6
78	Method for quantitative assessment of transformer oilâ€paper insulation nonâ€uniform ageing parameters based on frequency domain dielectric response. IET Science, Measurement and Technology, 2022, 16, 118-129.	0.9	6
79	Dual-calibration coefficient: a more accurate protocol for simultaneous determination of superoxide and hydrogen peroxide in human HepG2 cell extracts. Science China Chemistry, 2015, 58, 825-829.	4.2	5
80	Conditional cube attack on round-reduced River Keyak. Designs, Codes, and Cryptography, 2018, 86, 1295-1310.	1.0	5
81	Improved Integral Attacks on SIMON32 and SIMON48 with Dynamic Key-Guessing Techniques. Security and Communication Networks, 2018, 2018, 1-11.	1.0	5
82	TiO2 hollow spheres with surface-rich Ti3+ under Pd-catalyzed hydrogenation for improved visible-light photocatalysis. Journal of Nanoparticle Research, 2019, 21, 1.	0.8	5
83	One-pot green extraction of high charge density cellulose nanocrystals with high yield for bionanocomposites. Journal of Materials Science, 2021, 56, 12212-12223.	1.7	5
84	Enhancing the Removal of Sorbed Crude Oil from Soil Through Multiple Oxidation Steps in Stepwise Fenton Processes. Soil and Sediment Contamination, 2018, 27, 369-382.	1.1	4
85	Low Cost and Simple PMMA Nozzle Fabrication by Laser Cutting and PDMS Curing Bonding. International Journal of Precision Engineering and Manufacturing, 2021, 22, 139-146.	1.1	4
86	An "all-in-one―strategy based on the organic molecule DCN-4CQA for effective NIR-fluorescence-imaging-guided dual phototherapy. Journal of Materials Chemistry B, 2021, 9, 5785-5793.	2.9	3
87	The study of electrohydrodynamic printing by numerical simulation. Journal of Electrical Engineering, 2020, 71, 413-418.	0.4	3
88	Black wattle tanninâ€immobilized mesostructured collagen as a promising adsorbent for cationic organic dyes (methylene blue) removal in batch and continuous fixedâ€bed systems. Journal of Applied Polymer Science, 2022, 139, .	1.3	3
89	The fabrication of integrated and three-layer SU-8 nozzles for electrohydrodynamic printing. Microfluidics and Nanofluidics, 2020, 24, 1.	1.0	2
90	Novel phthalocyanine-based micelles/PNIPAM composite hydrogels: spatially/temporally controlled drug release triggered by NIR laser irradiation. New Journal of Chemistry, 2020, 44, 8705-8709.	1.4	2

#	Article	IF	CITATIONS
91	The Fabrication of Polymethyl Methacrylate Nozzles for Electrohydrodynamic Printing. Journal of Nanoscience and Nanotechnology, 2021, 21, 1735-1741.	0.9	2
92	A novel water-soluble phthalocyanine-based organic molecule for the effective NIR triggered dual phototherapy of cancer. New Journal of Chemistry, 2022, 46, 6353-6359.	1.4	2
93	Improved integral attacks without full codebook. IET Information Security, 2018, 12, 513-520.	1.1	1
94	A Novel Room-Temperature Bonding Method Based on Electrohydrodynamic Printing. Journal of Nanoscience and Nanotechnology, 2021, 21, 1672-1677.	0.9	0
95	Dietary with proper ratio of alphaâ€linolenic acid to linoleic acid enhanced the unsaturated fatty acids deposition of Chinese perch ( <i>Siniperca Chuatsi</i> ). Aquaculture Nutrition, 2021, 27, 73-85.	1.1	0
96	The effect of maternal polycyclic aromatic hydrocarbons exposure and methylation levels of congenital heart diseases andidate genes on the risk of congenital heart diseases. Prenatal Diagnosis, 2022, 42, 1142-1154.	1.1	0